# Energy Isosbestic Points in Third-Row Transition Metal Alloys

**Eugeny Todorov,[a] Matthew Evans,[a] Stephen Lee,*[a] and Roger Rousseau[b]**

**Abstract:** The total electronic energies of the six electrons per atom ($e^-$ per atom) alloys W, TaRe, HfOs, and YIr and the seven electrons per atom alloys Re, WOs, TaIr, HfPt, and YAu have been calculated in the local density approximation of density functional theory. When one considers common alloy structures such as atomically ordered variants of the body-centered cubic, face-centered cubic, or hexagonally closest packed structures and plots the total electronic energy as a function of the unit cell parameter, one finds for both the six and seven electrons per atom series energetic isosbestic points. An energetic isosbestic point corresponds to a critical value of the size parameter for which all members of the 6 or 7 $e^-$ per atom series of compounds have nearly identical total electronic energy. Just as in spectroscopy, where the existence of such isosbestic points is the hallmark of two compounds present in the mixture, an energy isosbestic point[1, 2] implies there are just two separate energy curves. For both series it is found that the total electronic energy can be viewed as the weighted sum of a purely covalent term and a purely ionic term. Two semi-quantitative models are proposed to account for these two separate energies. In the first model the total energy is viewed as the sum of the elemental structural energy plus an ionic energy based on the Born–Mayer ionic model. In the second model one considers within the confines of $\mu_2$-Hückel theory the evolution of the total electronic energy as the Coulombic $H_{ii}$ integrals change in value.

**Keywords:** ab initio calculations · alloys · bond theory · electronic structure · solid-state structures

## Introduction

The concept of the metallic-covalent/ionic bond lies at the heart of the chemistry. The idea rests on the following premises.[3–8] Pure covalent or pure metallic bonds can be understood by simple valence bond or molecular orbital theory. Pure ionic bonds are electrostatic in nature. In binary systems both pictures contain some fraction of the truth. The fraction itself depends on the electronegativity difference between the two elements. While this picture is useful in a qualitative understanding of bonding, it is not clear whether it is equally useful quantitatively. For example, in quantitative valence bond theory,[3] one associates one valence state with the covalent bond, a second state with the ionic bond, a resonance term for the interaction between these two states, and from the combination of these three one calculates the covalent–ionic bond energy. Not only must a resonance energy be calculated but one also has the limitation that for many systems, such as metals, it is diffcult in practice to calculate full valence bond energies. A simpler quantitative picture would be one in which the total energy of a binary system would be the weighted sum of the covalent and ionic energies of the system and in which both could be understood separately. For example we might expect that in Zintl compounds,[9, 10] systems in which there is a coexistence of primarily covalent and primarily ionic bonds, such a decomposition would be possible. The questions remain, are there other types of compounds for which such a decomposition is possible, and if so what is a convenient way to search for such families?

One approach to these questions is to find a series of compounds that differ primarily in either just the covalent or just the ionic energies. Differences in energies would therefore correspond to either purely covalent or purely ionic terms. The situation would be analogous to what one finds in spectroscopy when one measures the spectra of a series of mixtures. Just as in spectroscopy, the existence of isosbestic points is the hallmark of just two compounds present in the series of mixtures, an energy isosbestic point would be characteristic of two separate energy curves. Thus the question posed above, of whether the metallic-covalent/ionic bond

[a] Dr. S. Lee, Dr. E. Todorov, M. Evans
Department of Chemistry and Chemical Biology
Baker Laboratory, Cornell University
Ithaca, NY 14853-1301 (USA)
Fax: (+1) 607-255-0514
E-mail: sl137@cornell.edu

[b] R. Rousseau
Steacie Institute for Molecular Science
National Research Council of Canada,
100 Sussex Drive Ontario, K1N 0R6 (Canada)

  0947-6539/01/0712-2652 $ 17.50+.50/0 

can be thought of as the sum of a covalent energy and an ionic energy, can be reduced to a search for isosbestic points in related series of compounds.

In this paper we show that just such energy isosbestic points are found for third-row transition metal alloys. In particular we used local density approximation density functional theory (LDA-DFT) to calculate the total electronic energy as a function of the system's size.[11–23] We studied a series of pure elements and binary compounds in which the average number of valence electrons per atom ($e^-$ per atom) is constant. Thus W, TaRe, HfOs, and YIr each have an average of six electrons per atom. For the pure element W, bonds are purely metallic-covalent in character. Differences in energy between pure tungsten and the three binary compounds are due largely to the differences in electronegativities between the binary pair of atoms. Across a variety of structures, both those plausible for metal alloys, such as atomically ordered variants of face-centered cubic (fcc), body-centered cubic (bcc), and hexagonally closest packing (hcp), and those implausible for alloys, such as the rock salt structure and molecular dimers, isosbestic-type points are found across this series of four compounds. We similarly study series of compounds in which either the atomic parameters or unit cell parameters are continuously varied. In these cases we find isosbestic lines or surfaces. Equally clear isosbestic points are found for these same structures where one considers the parallel seven electrons per atom series, Re, WOs, TaIr and HfPt. These results strongly suggest that for the third-row transition metal alloys the total electron energy can be decomposed into metallic-covalent and ionic parts. We interpret these two separate energies by using both the Born–Mayer model for the ionic term[24] and $\mu_2$ molecular orbital theory[25–28] for both covalent and ionic contributions.

## Computational Methods

**LDA-DFT**: The total electronic energy is calculated iteratively from Equation (1) in which $\psi_i$ are the doubly occupied orbitals, $\rho(r)$ is the

$$E = 2\frac{-h^2}{2m}\sum_i \int \psi_i \nabla^2 \psi_i \mathrm{d}r + \int V_{\mathrm{ion}}\rho(r)\mathrm{d}r + \frac{e^2}{2}\int\frac{\rho(r)\rho(r')}{|r-r'|}\mathrm{d}r\mathrm{d}r' + E_{\mathrm{xc}}[\rho(r)] + E_{\mathrm{ion}}(\{R_\mathrm{I}\}) \quad (1)$$

electronic density, $V_{\mathrm{ion}}$ is the electrostatic ion–electron potential, $E_{\mathrm{ion}}$ is the electrostatic ion–ion potential, and $E_{\mathrm{xc}}$ is the exchange-correlation functional. In the LDA approximation the $E_{\mathrm{xc}}$ term is set [Eq. (2)], in which $\varepsilon_{\mathrm{xc}}$ is the exchange correlation energy of a homogeneous electron gas.

$$E_{\mathrm{xc}}[\rho(r)] = \int \varepsilon_{\mathrm{xc}}(r)\rho(r)\mathrm{d}V \quad (2)$$

Calculations were carried out with the Vienna Ab Initio Simulation Package (VASP)[29–32] by means of the ultrasoft Vanderbilt pseudopotentials[33] provided by the package. Plane-wave basis sets were used in the high-precision mode. This corresponds to plane-wave energy cut-offs of 186.9, 218.3, 235.3, 242.4, 252.0, 247.8, 239.2, and 224.6 eV for the third-row elements, starting with Hf and ending with Au. For Y the energy cut-off was 149.1 eV. The Brillouin zone sampling was done by Monkhost-Pack[34] **k** points grid ($15 \times 15 \times 15$ mesh). Partial occupancies of wavefunctions were made based on the tetrahedron method with Blöchl correction.[35] As a test of the numerical accuracy of our LDA-DFT calculations we also considered the general gradient approximation (GGA),[36] with the GGA pseudopotentials provided by the VASP package, as well as different partial occupancy algorithms. For these latter tests the algorithms considered include Fermi smearing, Gaussian smearing, and an order one Methfessel-Paxton correction.[37–39] The systems studied for these tests were those of W and TaRe, with a two atom cell: one atom at the origin and the second at $(x,y,1/2)$ for which $x$ and $y$ range in value from zero to one-half. The different total electronic energies from all the test calculations were within 0.005 eV per unit cell of the ones reported in this paper.

**$\mu_2$-Hückel theory**: In this tight-binding method[40–48] the total energy, $E_{\mathrm{T}}$, is expressed by Equation (3) in which $U(r)$ is a hard-core interatomic

$$E_{\mathrm{T}}(r) = U(r) - V(r) \quad (3)$$

repulsion energy, $V(r)$ is an attractive bonding energy, and $r$ is a parameter dependent on the size of the system. The total energy $E_{\mathrm{T}}$ can also be given by Equation (4) in which the integrals represent the repulsive and the

$$E_{\mathrm{T}} = \gamma\int_{-\infty}^{\infty}(E - E_{\mathrm{ave}})^2\rho(E,r)\mathrm{d}E + \int_{-\infty}^{E_{\mathrm{F}}} E\rho(E,r)\mathrm{d}E \quad (4)$$

attractive energy, respectively. Here $\rho(E,r)$ is the electronic density of the valence bands, $E_{\mathrm{F}}$ is the Fermi energy, $E_{\mathrm{ave}}$ is the average energy of the electronic density of states, and $\gamma$ is a proportionality constant. The density $\rho(E,r)$ is found from the diagonalization of the Hamilton matrix. Diagonal elements, $H_{ii}$, are set equal to prescribed Coulombic integral values, while off diagonal elements are based on the Wolfsberg-Helmholz approximation,[49] $H_{ij} = 1/2\,\mathrm{K}S_{ij}(H_{ii} + H_{jj})$. The parameter K is generally set to 1.75 and $S_{ij}$ is the overlap integral between the atomic orbitals $i$ and $j$. Atomic orbitals are assumed to be single or double $\zeta$ expansion Slater type orbitals. For the elemental systems the atomic parameters are the same ones used effciently in previous work on transition metal alloys.[27, 50] These are the parameters for Fe, $H_{ii}(4\mathrm{s}) = -9.10$ eV, $H_{ii}(4\mathrm{p}) = -5.32$ eV, $H_{ii}(3\mathrm{d}) = -12.60$ eV; $\zeta(4\mathrm{s}) = \zeta(4\mathrm{p}) = 1.9$, $\zeta_1(3\mathrm{d}) = 5.35$ (0.5505), $\zeta_2(3\mathrm{d}) = 2.00$ (0.6260). The parameter $\zeta$ was then determined from the condition that the total energy, $E_{\mathrm{T}}$, should have its global minimum at the experimental system size, $r = 2.88$ Å for bcc Fe. For the cases of six and seven electrons per atom, representing W and Re, the $\zeta$ parameters were determined to equal 0.6747 and 0.6546, respectively.

In this paper we model heteroatomic systems with two atoms of different electronegativities by changing Coulombic integrals while keeping the Slater exponents constant. We adopt the following simple scheme. The difference in $H_{ii}$ values between 4s, 4p, and 3d levels is a fixed constant: $H_{ii}(4\mathrm{s}) - H_{ii}(3\mathrm{d}) = 3.50$ eV and $H_{ii}(4\mathrm{p}) - H_{ii}(3\mathrm{d}) = 7.28$ eV. We assume that the difference in $H_{ii}$ values for the two atom types is 6 eV. There are, therefore, two undetermined numbers: the average $H_{ii}$ value for the two different atomic 3d orbitals and the proportionality constant $\gamma$.[51, 52]) We find these values by setting the isosbestic point for $\mu_2$-Hückel calculations to be the same as that found in LDA-DFT and by requiring that the asymptotic electronic energy at large interatomic separation is the same as that for the earlier homoatomic calculation. For the six electrons per atom systems the more electronegative element has an $H_{ii}(3\mathrm{d})$ of $-13.80$ eV, while $H_{ii}(4\mathrm{s})$ and $H_{ii}(4\mathrm{p})$ are $-10.30$ and $-6.52$ eV, respectively. The corresponding $H_{ii}$ parameters for the more electropositive atoms are exactly 6 eV higher in energy, that is, $-7.80$, $-4.30$, and $-0.52$ eV. For the systems with seven electrons per atom the two $H_{ii}$ parameters for the more electronegative atom are $-14.45$, $-10.95$, $-7.17$ eV. For the more electropositive atom these integrals are $-8.45$, $-4.95$, and $-1.17$ eV. The values for the parameter $\gamma$ for the heteroatomic six and seven electron systems were found to be 0.760 and 0.692.

**Born–Mayer theory**: In this model [Eq. (5)][24] for which we assume that

$$E_{\mathrm{total}} = E_{\mathrm{Coulombic}} + B\sum_{j\neq i} e^{-ar_{ij}} \quad (5)$$

all the atom sites corresponding to one atom are of charge $+1$ and those corresponding to the other atom are $-1$, and in which $E_{\mathrm{Coulombic}}$ is the electrostatic energy, $r_{ij}$ are the distances between nuclei $i$ and $j$, and $B$ and $a$ are constants. We find the values of $B$ and $a$ by requiring for TaRe that the energy is minimized at the experimentally observed cubic $a$ axis value of 3.26 Å. As discussed below we determine the values $B$ and $a$ by fitting to LDA-DFT calculations of TaRe with two atoms, at (0,0,0) and $(x,y,1/2)$; $0 \leq x,y \leq 0.5$ in a metrically cubic cell. This leads to the values of and a of 571.9

and 2.96, respectively. As we have arbitrarily assumed that charges are $\pm 1$, the total energy calculated by this method are in effect in arbitrary energy units. To derive real energy units one multiplies $E_{total}$ by a constant roughly equal to the charge on the cationic site.

## Results and Discussion

**Survey of isosbestic points**: We consider first the series W, TaRe, HfOs, and YIr. Ta and Re are the pair of elements before and after W in the periodic table, Hf and Os are the pair a step further removed, and Y and Ir are yet another step apart. The element Y is chosen instead of La as the atomic radius of Y more comfortably fits the observed progression of size in going from Y to Hf, Ta, W, and so forth. This is related to the lanthanide contraction.[53, 54]

In each of these four compounds there is an average of six valence electrons per atom, while the electronegativity differences for the four compounds from W to YIr increases from 0.0 to 0.4, 0.9, and 1.0 on the Pauling scale.[3] At room temperature and pressure each of these compounds is stable in the bcc or CsCl structure, illustrated in Figure 1.[55] The total

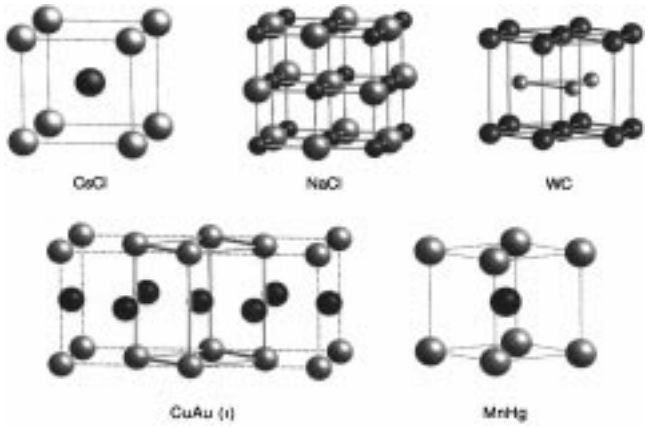


Figure 1. Crystal structures of CsCl, NaCl, WC, CuAu(I), and MnHg. For CuAu(I) an alternative choice of unit cell, which relates the structure to MnHg and CsCl, is shown.

electronic energy of these structures as a function of the *a* lattice constant is shown in Figure 2. Tungsten has the deepest energy minimum, and the energy minima become increasingly shallow across the series.

All four curves come to a common isosbestic point for an *a* lattice constant of 2.27 Å. The deviation along the abscissa from an ideal isosbestic point is 0.01 Å. The isosbestic point value of 2.27 Å is significantly shorter than the equilibrium lattice constants for YIr and W, 3.400 and 3.165 Å, respectively.[55] It therefore corresponds to a distance that is unrealistically short when compared with experimentally observed distances. One might, therefore, at first not ascribe any importance to the existence of this equivalence point. However, it can be seen that the softness of the energy curves at the unrealistic distances to the left of the isosbestic point

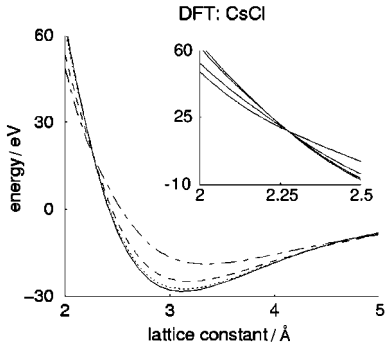


Figure 2. Total electronic energy of binary transition metal alloys in the CsCl structure as a function of the *a* lattice parameter. W, TaRe, HfOs, and YIr are represented by solid, dotted, dashed and dash-dotted lines, respectively. The insert shows the region of the isosbestic point.

corresponds quite closely to the softness found for the experimentally pertinent distances to the right of this point.

Furthermore, all such energy curves can be fit approximately to the Rose universal energy curve.[56] The latter is a three parameter curve found to exemplify an energy–length relationship for a large number of systems. As all Rose curves can be described by three parameters and as all the curves in Figure 2 share a common point, we must be restricted to just two parameters in describing this sub-family of the Rose curves. It turns out that this parameter subset may be viewed as a two-dimensional subspace. Basis functions for the subspace may be taken to be the W curve and the difference in energy between the W curve and the YIr curve. In Figure 3 we show linear combinations of the W and YIr curves fit to reproduce the TaRe and HfOs LDA-DFT results. A comparison of Figures 2 and 3 show that these linear combinations

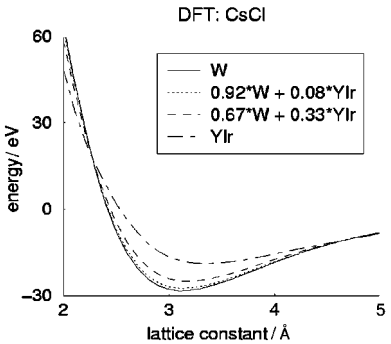


Figure 3. Linear combinations of the LDA-DFT electronic energy W and YIr curves (solid and dash-dotted lines) similar to the LDA-DFT TaRe and HfOs energy curves of Figure 2.

provide a qualitative fit to the full LDA-DFT results. In the same manner we may consider other reasonable alloy structures. For example, we may consider the CuAu(I) ordered variant of fcc and the WC variant of the hcp packing. These structures are also illustrated in Figure 1. While CuAu(I) is of tetragonal symmetry, we have chosen a metrically cubic unit cell (also shown in Figure 1) for our calculations. Similarly in our calculations of ordered hcp phases we choose the ideal *c*/*a* ratio of 1.633, the ratio at which each atom has twelve equidistant nearest neighbors. In Figures 4 and 5 for both the



0947-6539/01/0712-2654 $ 17.50+.50/0 *Chem. Eur. J.* **2001**, *7*, No. 12

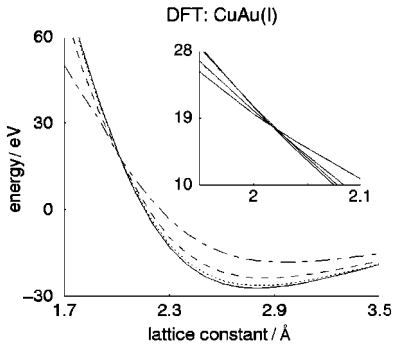


Figure 4. Total electronic energy of binary transition metal alloys in the CuAu(I) structure, an ordered variant of fcc structure, as a function of the *a* lattice parameter. See caption of Figure 2 for curve definitions.

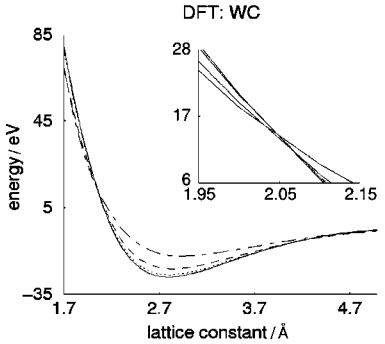


Figure 5. Total electronic energy of binary transition metal alloys in the WC structure, an ordered variant of hcp structure, as a function of the *a* lattice parameter. See caption of Figure 2 for curve definitions.

CuAu(I) and WC structures, we plot the total electronic energy as a function of the lattice parameters. As in the CsCl study we find the deepest minima for W and the shallowest for YIr. Again nearly perfect isosbestic points are observed (see inserts of Figures 4 and 5). The error for the former is approximately 0.02 Å, while for the latter it is 0.03 Å.

Finally, for the sake of interest we consider two structures not compatible with structures ordinarily found for transition metal alloys. The first one is the rock salt structure in which every atom has only six nearest neighbors, half that found in ordinary transition metal1 alloys. The second one is the molecular structure composed of a dimer of transition metal atoms. Here the coordination number is just one. As the inserts of Figures 6 and 7 show, the deviation from ideal

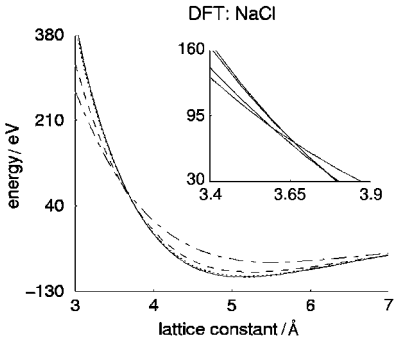


Figure 6. Total electronic energy of binary transition metal alloys in the NaCl structure as a function of the *a* lattice parameter. See caption of Figure 2 for curve definitions.

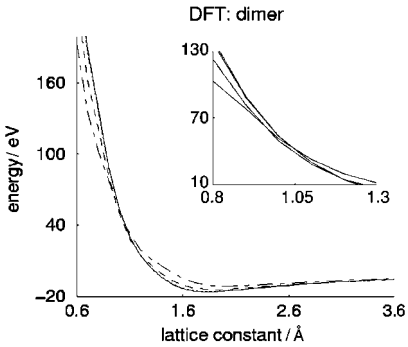


Figure 7. Total electronic energy of transition metal dimer molecules as a function of the interatomic distance *a*. See caption of Figure 2 for curve definitions.

isosbestic points is quite large for these systems. The error is greatest for the case of the molecular dimer, 0.3 Å. These results suggest that the occurrence of an energy isosbestic point holds best for high coordination number structures as are found in true alloy structures. Isosbestic points will be less ideal and even non-existent for insulating structures with lower coordination number.

**The CsCl, CuAu(I), and MnHg structures**: Among the simple structures most related to transition metal alloys with 6–7 $e^-$ per atom are the tetragonal CuAu(I) and MnHg structures.[55] Both structures can be described in a tetragonal cell with just two atoms per unit cell (see Figure 1). One atom type is located at the corner of the unit cell, while the second atom is at the body center. The difference in the structures comes from the *c*/*a* ratio. For CuAu(I) this ratio is near $\sqrt{2}$ and, hence, CuAu(I) is an atomically ordered variant of fcc, while for MnHg the *c*/*a* ratio is near unity and, thus, MnHg is a slight tetragonal distortion of the cubic CsCl structure. Metal alloys with 6–7 $e^-$ per atom found in the CuAu(I) structure are TiRh, TiAg, VRh, VIr, NbRh, and NbIr, while for the MnHg type examples include LaAg, LaCd, TbCu, TiIr, NbRu, and TaRu.[55] These two structure types are, therefore, members of a more general structure type, a primitive tetragonal cell with one atom type at the corner and the second atom in the body center. In this amalgamated structure type there are just two variable parameters, the *a* and *c* axis lengths.

In the previous section we considered structure types with a single structural parameter, either the cell axis or the bond length. For each structure type we found energetic isosbestic points. With the CuAu(I)/MnHg structure at each *c*/*a* ratio one may find a corresponding single isosbestic point. In Figure 8 we show two such isosbestic points for the 6 $e^-$ per atom series, W, TaRe, HfOs, and YIr for $c/a = 0.80$ and $c/a = 1.20$. Together with the earlier 6 $e^-$ per atom results for CsCl ($c/a =$ 1.00, Figure 2) and the ordered fcc structure ($c/a = 1.41$, Figure 4), these results suggest that for all *c*/*a* ratios there is an isosbestic point. The locus of these individual isosbestic points is a one-dimensional curve, an isosbestic line. This line is found at cell volumes slightly less than 12 Å per unit cell. In Figure 9 we plot the electronic energy as a function of the *c*/*a* ratio for the fixed volume of 11.775 Å. Were this volume to correspond exactly to the isosbestic line, all four curves would

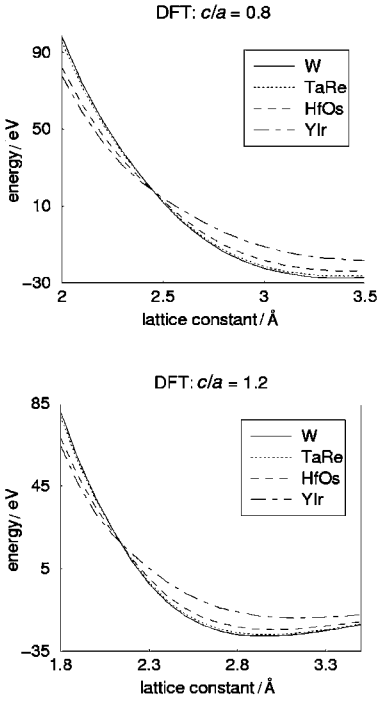


Figure 8. Total electronic energy of binary transition metal alloys in the MnHg structure as a function of the *a* lattice parameter. The ratio between the *c* and *a* axes is arbitrarily fixed at the values of 0.8 (top) and 1.2 (bottom).

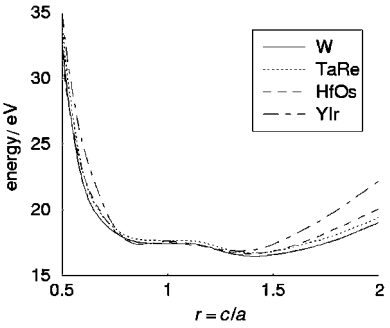


Figure 9. The electronic energy at a fixed volume of 11.775 Å as a function of the *c*/*a* ratio.

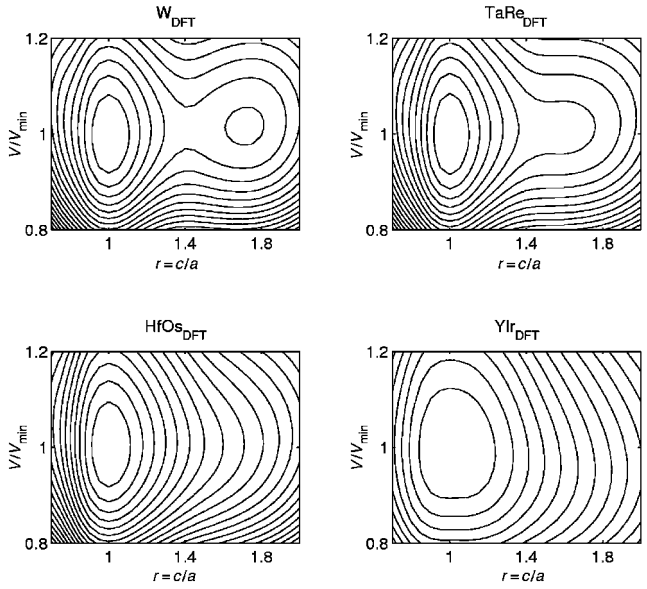


Figure 10. Electronic energies of the 6 $e^-$ per atom compounds plotted as contour maps. The two variables are the *c* to *a* axes ratio and the cell volume. The latter is expressed as the ratio of the cell volume to $V_{min}$, the volume of the structure at the global energetic minimum. Thus points corresponding to the experimentally observed bcc elemental structures are at *r* and $V/V_{min}$ both equal to one.

lie on top of one another. Between *c*/*a* values ranging from 0.75 to 1.50 the curves deviate from one another by 0.3 to 0.5 eV. For *c*/*a* ratios below 0.75 the errors become larger. This result correlates to our findings in the previous section. There we found isosbestic points for true alloy structures were more perfect than those for lower coordination geometries. For *c*/*a* ratios from 0.8 to 1.5, the number of atoms within metallic bonding distances range from 10 to 14. For unreasonably low *c*/*a* ratios of 0.6, however, nearest neighbors are only along the *c* axis. At such low *c*/*a* ratios, the structure can be viewed primarily as polymeric, with two coordinate metal chains running parallel to the *c* axis. Similarly at unreasonably high *c*/*a* ratios of 1.7, nearest neighbors are only in the *ab* plane. The structure is primarily a square net, that is, each atom has only four nearest neighbors. It is for such chemically unreasonable alloy geometries that the validity of the isosbestic point begins to break down.

A comparison of the individual surfaces is instructive. In Figure 10 we plot the electronic energy of the four compounds W, TaRe, HfOs, and YIr as contour maps. In these graphs the abscissa is the ratio of the *c* and *a* lattice parameters and the ordinate is the ratio of unit cell volume to $V_{min}$, the cell volume corresponding to the global energy minimum structure. Both abscissa and ordinate are therefore unitless and allow for ready comparison of experimental systems of different equilibrium size. In all four cases shown in Figure 10 the global minimum is found for a *c*/*a* ratio of one. This corresponds to the bcc or CsCl structure. It is indeed this structure that is observed experimentally. Of greater interest perhaps is the local minimum found for *c*/*a* ratio of 1.7 for elemental W. In the next compound in the series, TaRe, this local minimum is much softer and has shifted to a *c*/*a* ratio of 1.6. In the remaining two systems this minimum has disappeared. For YIr, besides the global minimum, the overall electronic surface is essentially featureless.

We may rationalize these results in two ways. In the first approach one uses the Born–Mayer model of ionic interactions. Here the attractive potential is based on the Coulombic electrostatic interaction, while the repulsive potential is a hard core potential, modeled as an exponential term, $e^{-ar}$. In such a model, structures are optimal when one brings opposite charges close together, while keeping like charges far apart. The model generally favors high-symmetry over low-symmetry structures. With the MnHg/CuAu(I) structure type the optimal structure is for $c/a = 1.0$ with cubic symmetry. At this value, the structure is actually in the CsCl arrangement in which all first nearest neighbors are between atom types of opposite charge and only second nearest neighbors are of like charge. We therefore expect in an ionic model both that the CsCl structure would be the energetically preferred structure and that electronic energy surface would be quite smooth.



0947-6539/01/0712-2656 $ 17.50+.50/0 *Chem. Eur. J.* **2001**, *7*, No. 12

In the upper left corner of Figure 11 we show the results of such a Born–Mayer calculation. The overall shape is the one expected. The surface is quite smooth, and there is only a single minimum, which corresponds to the CsCl structure. Comparing the Born–Mayer surface of Figure 11 with the energies of the W, TaRe, HfOs, and YIr series in Figure 10, we see that the agreement between the ionic model and the actual LDA-DFT electronic energy surfaces is best for the more ionic YIr and HfOs systems and worse for the non-ionic W system. The TaRe potential can then be thought of a linear combination of the purely metallic-covalent W surface and the purely ionic Born–Mayer energy surface. In Figure 11 we show that such linear combinations do result in energy surfaces similar to these of TaRe, HfOs, and YIr. Thus the TaRe DFT surface of Figure 10 is well approximated by the linear combination of 0.81 times the W DFT surface and 0.19 times the Born–Mayer surface, as is shown in the upper right of Figure 11. Agreement is worse for YIr, which is best modeled as 0.44 times the W DFT surface plus 0.56 times the Born–Mayer energy surface as is shown in the lower right of Figure 11.

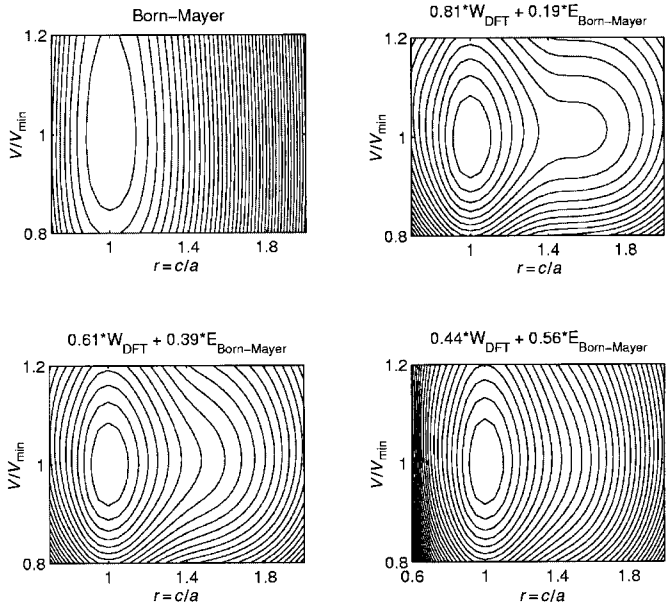


Figure 11. Linear combinations of the ionic Born–Mayer energy, $E_{\text{Born–Mayer}}$ (upper left contour), and the covalent DFT energy of tungsten, $W_{DFT}$. The results qualitatively correspond to the DFT energies of TaRe, HfOs, and YIr shown in Figure 10.

One may however take an alternative approach in rationalizing the results of Figure 10. In this approach we use a tight-binding model to calculate the metallic-covalent bond energy. We use here the $\mu_2$-Hückel model, a model in which a repulsive energy, proportional to the variance of the valence electron density of states, is added to the attractive Hückel Hamiltonian. The model has been proven successful in many areas in which the understanding of the electronic structure is of interest. It has given intelligible insights into the structural stability of elements, organic and organometallic molecules, cluster compounds,[57] and networks of main group intermetallics.[58] Recently the $\mu_2$-Hückel model has been used in rationalization of alloy structures,[59] understanding of the electronic structure and stability of thermoelectrics,[60] or of alloys at high pressure.[61]

This model is described in the section on Computational Methods. As $\mu_2$-Hückel theory atomic parameters have not been established for third-row transition elements, we use the previously characterized first-row parameters. We choose the equilibrium size to be the one that corresponds to bcc. However, as we plot in our contour map $c/a$ at $V/V_{\text{min}}$, two unitless quantities, the results from the first-row calculations can be directly compared to the third-row LDA-DFT results.

Using this model results in the energy surface shown on the left side of Figure 12. For $c/a$ values above 0.7 the $\mu_2$-Hamiltonian gives an electronic energy surface in partial agreement with the LDA-DFT results. The $\mu_2$-Hamiltonian has a global minimum for $c/a = 1.0$, the CsCl structure, and a second local minimum at the same volume as the global minimum but for $c/a = 1.6$. For values below 0.7, the $\mu_2$-Hückel surface fares worse. This breakdown can be rationalized. The $\mu_2$ model is most accurate when comparing structures with comparable coordination number. It has been proven to give qualitative and semiquantitative energies when contrasting one alloy structure with another. It is not as useful when comparing the two coordinate linear chain structure found for $c/a = 0.6$ to the twelve and fourteen coordinate fcc and bcc structures. The $\mu_2$-Hamiltonian becomes inaccurate exactly in region where the energy isosbestic points also deteriorate.

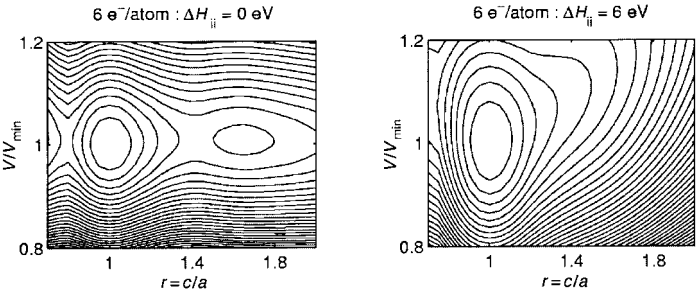


Figure 12. $\mu_2$-Hückel energies for transition metal alloys in the MnHg structure type an element ($\Delta H_{ii} = 0$ eV) and a binary compound ($\Delta H_{ii} = 6$ eV) each with an average of 6 $e^-$ per atom. The results are in partial agreement with the DFT energies of W and TaRe shown in Figure 10.

We now consider the binary alloys within the same model. In Hückel theory there are two types of atomic parameters: the Coulombic integrals, which model the electronegativity of the atoms, and the Slater exponents, which model the atomic size. In the series of compounds W, TaRe, and HfOs the differences in the electronegativity between constituent atoms is expected to be more dominant than size factors. We therefore vary only the Coulombic parameters, keeping the Slater exponents constant throughout. Thus we consider the following model calculation. We shift the Coulombic integrals for the valence s, p, and d orbitals of one atom type so that they lie 6 eV higher than their counterparts in the other atom type. This will have two effects on the $\mu_2$-Hückel energies. As we use the Wolfsberg–Helmholz approximation, off-diagonal matrix elements will become smaller in value. Secondly, as the interaction between two orbitals at different

energies is inversely proportional to the original difference in orbital energies, bonding energies will also become smaller. The net result is that a tight-binding theory going from a metallic-covalent system to a more ionic one invariably results in a softening of the overall energy surface. This is a phenomenon we have observed in the previously discussed LDA-DFT calculations. The question still remains as to how one should determine the proportionality constant $\gamma$, which controls the relative strengths of the attractive and repulsive portions of the $\mu_2$-Hamiltonian. The results previously discussed in this paper suggest the following approach. If we require in Hückel theory that there should also be an isosbestic point at the same distance as that found in the LDA-DFT calculations, and further require that at large volumes both the elemental system and the binary systems have the same $\mu_2$-Hückel asymptotic energies, we can then determine both values of $\gamma$ and the average atomic orbital energy.

In Figure 13 we show that such a model does capture the overall qualitative results seen earlier in Figures 2–8. There is a softening of the energy surface in going from more covalent

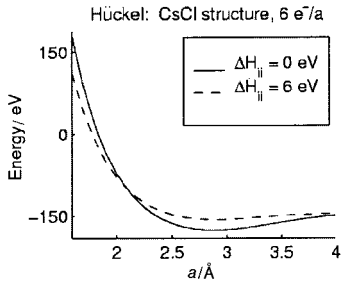


Figure 13. $\mu_2$-Hückel electronic energy of 6 $e^-$ per atom transition metal compounds in the CsCl structure as a function of the *a* lattice parameter.

to more ionic systems. The electronic energy surface corresponding to this calculation is shown on the right side of Figure 12. In comparing the two contour maps in Figure 12 we can see that the result of the change in Coulombic integrals is the loss of the local minimum at high *c*/*a* ratio with retention of the global overall minimum for $c/a = 1.0$. The second minimum shifts from a value of $V/V_{min}$ of 1.6 for $\Delta H_{ii} = 0$ eV to a larger $V/V_{min}$ value for $\Delta H_{ii} = 6$ eV. The former result matches the findings of the LDA-DFT calculations in Figure 10. The latter result does not. Nevertheless, it may be seen that the $\mu_2$-Hückel results capture many of the essential features of the LDA-DFT calculations.

We are therefore left with two alternative ways of rationalizing the LDA-DFT calculations for W, TaRe, HfOs, and YIr. One can qualitatively account for the results either with a Born–Mayer model or with tight-binding theory. In order to distinguish between these alternative views, we need to find a series of compounds for which a tight-binding theory and a electrostatic model are not in agreement.

**Seven electrons per atom systems**: While 6 $e^-$ per atom binary transition metal alloys are primarily in the bcc structure type, above 7 $e^-$ per atom both closest packings and bcc structures are found. Thus low temperature TiPd, TiPt, VIr, VPt, NbRh, NbIr, TaIr, CrRh, MoRh, WIr, Tc, and Re, all with 7–7.5 $e^-$ per atom, are found in hcp, fcc, dhcp ("double" hexagonal close packing), or atomically ordered variants of these different closest packings.[55, 62, 63] By contrast low-temperature bcc phases or ordered variants of the bcc structure type include the 7 $e^-$ per atom REAg (RE = rare earth element) compounds, all the 7–7.5 $e^-$ per atom ScM (M = Group 10–12, except ScZn) and the 7.5 $e^-$ per atom low-temperature TiCu, TiAg, ZrAg, HfAg, and HfAu systems. The first two families form in the ordered bcc structure type CsCl and the last family is another ordered bcc structure, the TiCu type.

These results suggest that for small electronegativity differences between the constituent atoms the closest packed structures are preferred, while for large electronegativity differences the bcc arrangement is energetically more stable. We infer that the metallic-covalent part of the energy favors closest packing while the ionic energy favors the bcc structure.

Therefore, a study at 7 $e^-$ per atom systems allows one to examine the transformation from the metallic-covalent regime to the ionic regime. As in the previous section we consider the MnHg/CuAu(I) structure type for the 7 $e^-$ per atom series Re, WOs, TaIr, and HfPt. We choose this structure type as in changing the *c*/*a* ratio from 1.4 to 1.0 one passes from the cubic closest packing, which is more stable for small electronegativity differences between the constituent atoms, to the CsCl structure, which is more stable for high electronegativity differences.[64] In Figure 14 we show the electronic energy for this series of compounds as a function of the lattice constant for *c*/*a* ratio of 0.8 and 1.2. As in Figure 8, we see that

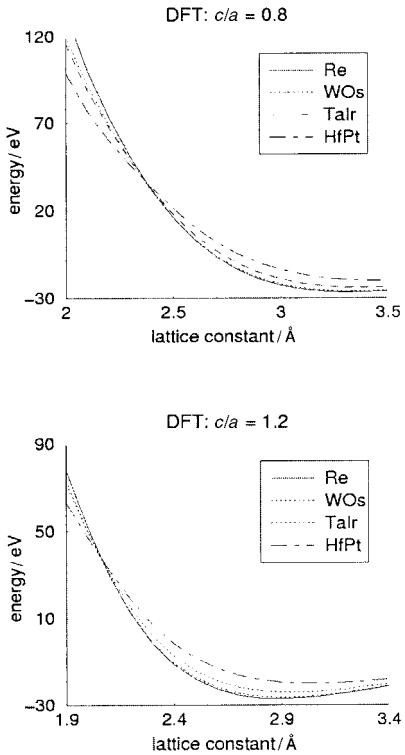


Figure 14. Total electronic energy of binary transition metal alloys in the MnHg structure as a function of the *a* lattice parameter. The ratio between the *c* and *a* axes is fixed at the values of 0.8 (top) and 1.2 (bottom).



0947-6539/01/0712-2658 $ 17.50+.50/0 *Chem. Eur. J.* **2001**, *7*, No. 12

the various surfaces intersect at a common isosbestic point. In Figure 15 we show the corresponding electronic energy contour maps. For Re one finds a global minimum at $c/a = 1.4$; the fcc structure is most stable. It is known experimentally that Re is indeed most stable as a closest packing. A second shallow minimum is found for $c/a$ ratios less than 1.0. For the next member of this series of compounds, WOs, the global minimum is still fcc; however, the local minimum at $c/a = 0.9$ is more pronounced. For TaIr, the elements two groups to the left and to the right of Re in the periodic table, this second local minimum, now at $c/a = 0.85$ is even more pronounced. The CsCl structure, in which $c/a = 1.0$, corresponds to a marked saddle point. For HfPt these two minima begin to fuse together into one common rather soft energy well. Finally, if we include the next possible member of the series, YAu, this now single minimum becomes well localized at $c/a = 1.0$. Indeed, YAu crystallizes in the CsCl structure type.

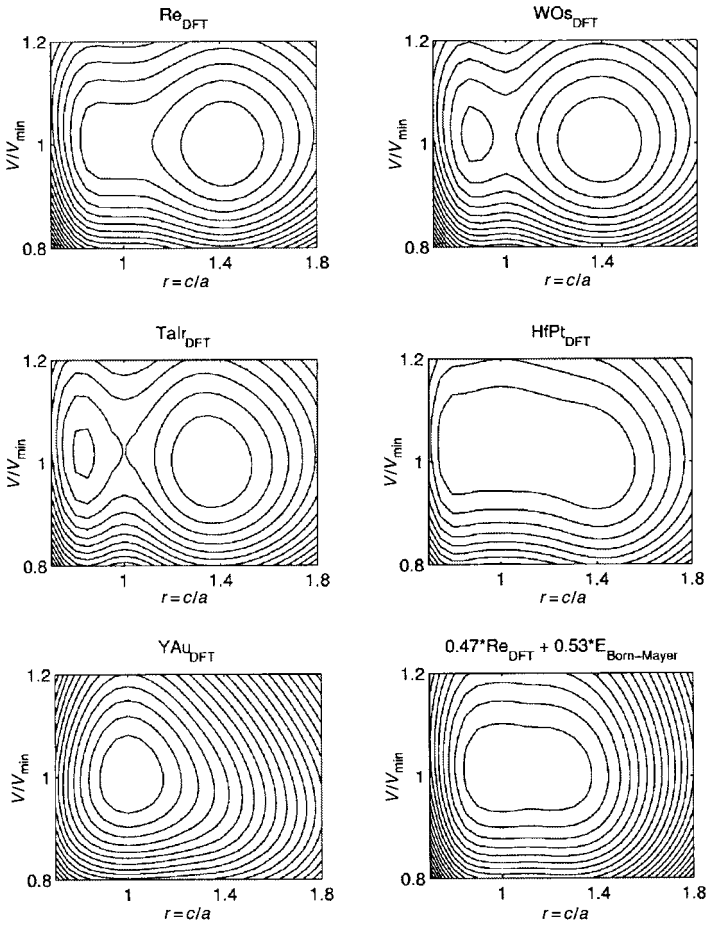


Figure 15. Electronic energies of the 7 $e^-$ per atom compounds plotted as contour maps. In the lower right corner a linear combination of the DFT energy of the covalent Re and the ionic Born – Mayer energy is shown as an approximate fit to the DFT energy of HfPt shown in the Figure as $HfPt_{DFT}$.

We can use this data to assess the two pictures developed in the previous section for the rationalization of surface shape. In the first model we consider that the electronic energy is a linear combination of the Re energy surface, the upper left diagram in Figure 15 and the Born – Mayer ionic energy surface, the upper left diagram of Figure 11. Encouragingly, we see that the electronic energy surface for the end member of this series, YAu, resembles qualitatively the Born – Mayer surface of Figure 11. Both surfaces have only one minimum corresponding to the CsCl structure. However, the Born – Mayer surface has a greater energy dependence on the $c/a$ ratio than does the YAu surface. Just as in the previous section, we can take a linear combination of the Born – Mayer energy surface and the non-ionic Re LDA-DFT surface to produce the electronc energy surface shown in the last diagram of Figure 15. The qualitative agreement between the last contour in Figure 15 and the LDA-DFT result for HfPt is clear. However, it is not possible to simulate WOs and TaIr surfaces by such a linear combination. For these two systems the global minimum is at $c/a = 1.4$ and a local minimum appears at $c/a \approx 0.85$, while $c/a = 1.0$ corresponds to a saddle point. As the Re DFT energy surface has a minimum $c/a = 1.4$ and the Born – Mayer energy surface has a minimum at $c/a = 1.0$, it is not possible to combine these two surfaces and find a local minimum at $c/a \approx 0.85$.

We now turn to the second model, the $\mu_2$-Hückel model. We show on the left side of Figure 16 the energy surface for 7 $e^-$ per atom by using the same atomic parameters used in the previous calculation, in which $\gamma$ was determined again so that the bcc structure should have a lattice constant of bcc Fe. There is a reasonable correspondence between the $\mu_2$-Hückel results and those for elemental Re. As in the LDA-DFT calculations, there is a global minimum for $c/a = 1.4$, a saddle point at $c/a = 1.0$, and a very shallow local minimum just below $c/a = 1.0$.

As in the previous section, we can model different atom types by shifting the Hückel Coulombic integrals for one atom type s, p, and d orbitals so that they lie 6 eV higher relative to the energy of the other atom's correpsonding atomic orbitals. In Figure 17, we see the general softening of the electronic energy as a function of lattice constant this model engenders. In Figure 16 on the right side we show the corresponding energy surface contour. Just as was observed for WOs and TaIr, while the global minimum remains at $c/a = 1.4$, a second

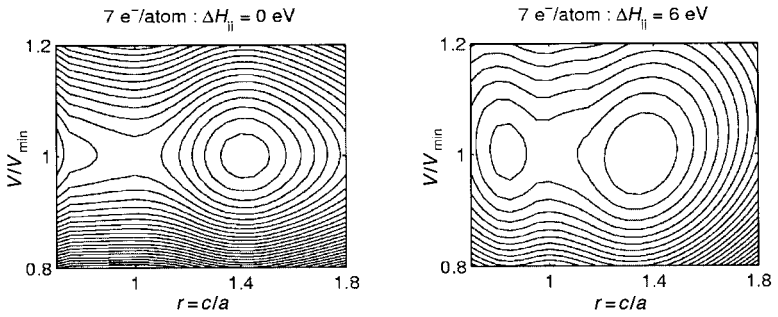


Figure 16. $\mu_2$-Hückel energies for transition metal alloys in the MnHg structure type an element ($\Delta H_{ii} = 0$ eV) and a binary compound ($\Delta H_{ii} = 6$ eV) each with an average of 7 $e^-$ per atom. The results are in qualitative agreement with the DFT energies of Re, WOs, and TaIr shown in Figure 15.

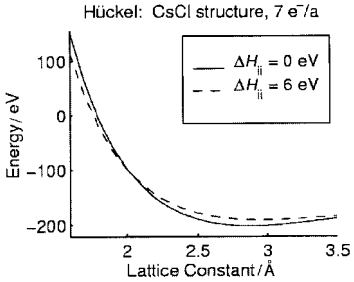


Figure 17. $\mu_2$-Hückel electronic energy of 7 e$^-$ per atom transition metal compounds in the CsCl structure as a function of the $a$ lattice parameter.

pronounced local minimum appears at $c/a = 0.85$. There is therefore qualitative agreement between $\mu_2$-Hückel theory and the LDA-DFT results for the first members of this series, Re, WOs, and TaIr. But this same $\mu_2$-Hückel theory breaks down for the latter members of the family. This breakdown is first seen in the use of the Wolfsberg–Helmholz approximation. While we can shift the atomic orbitals by 6 eV relative to one another, even greater shifts would lead to positive Coulombic integrals for some of the atomic orbitals. Such positive values are meaningless.

Perhaps more importantly there is a qualitative breakdown in the $\mu_2$-Hückel Hamiltonian. In the limit of large differences in Coulombic integrals, off-diagonal terms in the tight-binding model tend to zero. Thus, in the limit of an extremely electropositive element being mixed with an equally electronegative one, there is no energy of interaction in the tight-binding system. Clearly in such a system there must be a considerable ionic term, as the electronegative atom will have accumulated electron charge from the electropositive atom. The solution is clear. One needs to combine elements of the two pictures to establish a qualitatively persuasive picture of the electronic energy. The $\mu_2$-Hückel theory provides information for the first members of the series such as Re, WOs, and TaIr, the Born–Mayer model is valid for YAu, and a linear combination of the two is valid for HfPt. These results suggest the following picture for the bonding in binary third-row transition metal alloys. The electronic energy can be thought of qualitatively and semiquantitatively as the sum of separable metallic-covalent and ionic energies. The pure metallic-covalent portion of the energy can be modeled by a tight-binding model such as $\mu_2$-Hückel theory. The ionic portion of the energy is more complex. While for large differences in electronegativity the Born–Mayer model is pertinent, for smaller differences one needs to turn to alternative pictures such as that found in $\mu_2$-Hückel theory itself. It should be noted that in Hückel theory one can separate the energy effects of the metallic-covalent portion from the ionic effects. For example, one can use a moment expansion[26] and formally divide the contribution from these two portions. Therefore, the ionic energy can be expressed as a separate calculable entity.

**Atomic parameter variation**: In the previous two sections of this paper we noted the continued presence of energetic isosbestic points as one continuously varies the ratio of the cell parameters. We may also consider the electronic energy as a function of atomic parameters. Perhaps the simplest system we can consider is the two atom cell in which the cell axes are metrically cubic. We can place two atoms into the cell; the first atom is placed at the origin, while the second atom is located at $(x,y,1/2)$ for which $x$ and $y$ are variable. For $x = y = 1/2$ the overall structure is the cubic CsCl, while for $x = y = 0$ the structure is tetragonal with infinite linear chains of atoms running in the $c$ direction. Only at values near $x = y = 1/2$ does the structure remain a high-coordinate one and only here do we expect to see marked energetic isosbestic points. In Figure 18 we show the energy curves for $x = y = 0.45$ and $x = 0.4$, $y = 0.5$ for 6 and 7 e$^-$ per atom. The energetic isosbestic points are clear.

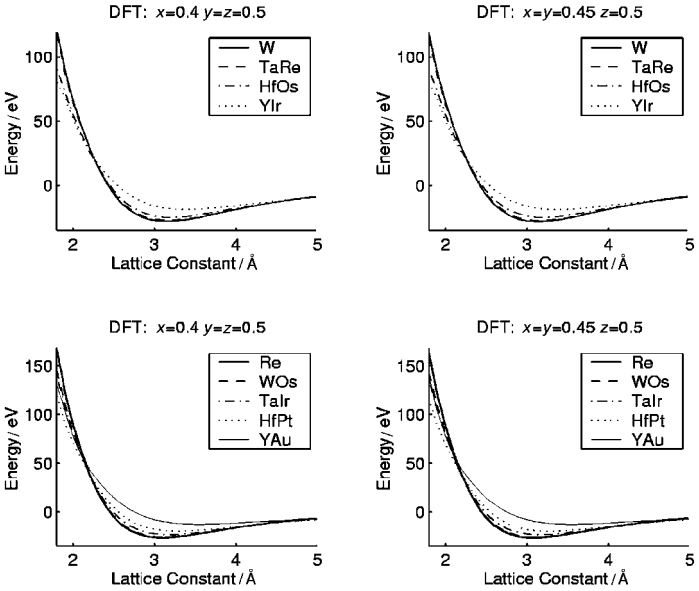


Figure 18. DFT energy curves for metrically cubic systems, with one atom at the origin (0,0,0) and the second one arbitrarily fixed at $(x,y,1/2)$, as a function of the lattice parameter. For the left two figures, $x = 0.4$ and $y = 0.5$, while for the right two, $x = y = 0.45$.

We plot in Figure 19 the total electronic energy surface for the five 7 e$^-$ per atom systems: Re, WOs, TaIr, HfPt, and YAu. It may be seen that all five surfaces have a similar shape. The energy scale is different. The energy minimum is deeper for Re and shallowest for YAu.

These results suggest that both the covalent and ionic energies in these systems have similar energetic surfaces. As we do not need to a priori deduce the relative contributions of these two different energies, we may directly model this surface with either a purely covalent or a purely ionic energy. These surfaces allow us to find the empirical parameters necessary to complete the Born–Mayer expression. The best Born–Mayer model fit to the experimentally observed surface is shown in Figure 19. The qualitative agreement between the Born–Mayer model and the LDA-DFt model is clear.

It is unfortunately not possible to model these same LDA-DFT results with $\mu_2$-Hückel theory. This latter theory breaks down when comparing such dissimilar coordination environments, such as the two nearest neighbors per atom structure for $x = y = 0$ and the fourteen near-neighbors geometry for $x = y = 1/2$.



0947-6539/01/0712-2660 $ 17.50+.50/0 *Chem. Eur. J.* **2001**, *7*, No. 12

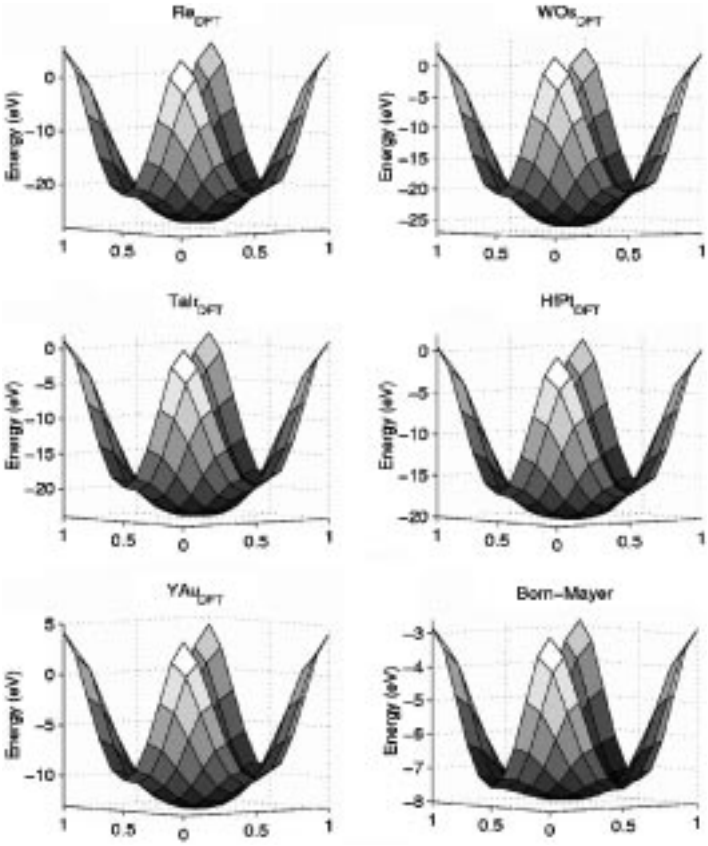


Figure 19. Energy surfaces for metrically cubic systems with one atom at the origin (0,0,0) and the second one at ($x$,$y$,1/2) as a function of atomic parameters $x$ and $y$. At the bottom right corner is the Born – Mayer energy surface.

## Conclusion

When chemists think of chemical bonds it is generally supposed that main group bonding is simpler than transition metal bonding, molecules are easier to study than extended solids, and low-coordination environments, such as the tetrahedral or octahedral geometries, are more basic than the high-coordinate cuboctahedral or anticuboctahedral environments. One might then suppose the paradigm of the covalent and the ionic bond would be most effective in the study of low coordination number main group molecules. In this paper we find the converse. High-coordination number transition metal alloys prove to have a particularly transparent form for their covalent-metallic and ionic energies. For these systems the total electronic energy is a sum of separable covalent-metallic and ionic energies.

In hindsight we can see some of the factors responsible. In main group systems both the s and p bands are essential to the bonding. Furthermore the degree of s and p mixing depends on whether the geometry is linear, trigonal, or tetrahedral. Therefore, a binary main group compounda already has four key parameters, the atomic energes of the two atoms, and valence s and p orbitals. By contrast transition metal alloys bonding is dominated by the d orbitals. Binary transition metal alloys have only two key parameters, the two atomic valence d orbital energies. Two parameter systems can lead to just two functions. It is only in cases like this that energy isosbestic points, like the ones discussed in this paper, are possible.


[1] R. S. Drago, *Physical Methods in Chemistry*, Saunders, Philedelphia, **1977**.
[2] B. Najafi, G. Parsafar, S. Alavi, *J. Phys. Chem.* **1995**, *99*, 9248.
[3] L. Pauling, *The Nature of the Chemical Bond*, 3rd ed., Cornell University Press, Ithaca, NY, **1960**.
[4] A. E. van Arkel, *Molecules and Crystals in Inorganic Chemistry*, Interscience, New York, **1956**.
[5] J. A. A. Ketelaar, *Chemical Constitution: An Introduction to the Theory of the Chemical Bond*, 2nd ed., Elsevier, Amsterdam, **1958**.
[6] L. C. Allen, J. F. Capitani, *J. Am. Chem. Soc.* **1994**, *116*, 8810.
[7] D. G. Pettifor, *Bonding and Structure of Molecules and Solids*, Oxford University Press, New York, **1995**.
[8] W. P. Anderson, J. K. Burdett, P. T. Czech, *J. Am. Chem. Soc.* **1994**, *116*, 8808.
[9] E. Zintl, J. Goubeau, W. Dullenkopf, *Z. Phys. Chem. Abt. A* **1931**, *154*, 1.
[10] *Chemistry, Structure and Bonding of Zintl Phases and Ions* (Ed.: S. Kauzlarich), VCH, New York, **1996**.
[11] P. Hohenberg, W. Kohn, *Phys. Rev. B* **1964**, *136*, 864.
[12] W. Kohn, L. J. Sham, *Phys. Rev. A* **1965**, *140*, 1133.
[13] R. O. Jones, O. Gunnarsson, *Rev. Mod. Phys.* **1989**, *61*, 689.
[14] F. Chu, T. E. Mitchell, S. P. Chen, M. Sob, R. Siegl, D. P. Pope, *J. Phase Equilib.* **1997**, *18*, 536.
[15] C. Zhang, P. Hu, A. Alavi, *J. Am. Chem. Soc.* **1999**, *121*, 7931.
[16] A. M. C. Wittborn, M. Costas, M. R. A. Blomberg, P. E. M. Siegbahn, *J. Chem. Phys.* **1997**, *107*, 4318.
[17] L. Vitos, A. V. Raban, H. L. Skriver J. Kollar, *Surf. Sci.* **1998**, *411*, 186.
[18] J. Kua, W. A. Goddard, *J. Am. Chem. Soc.* **1999**, *121*, 10928.
[19] G. Frenking, N. Fröhlich, *Chem. Rev.* **2000**, *100*, 717.
[20] P. Soderlind, L. H. Yang, J. A. Moriarty, J. M. Wills, *Phys. Rev. B* **2000**, *61*, 2579.
[21] U. Häussermann, S. I. Simak, R. Ahuja, B. Johansson, *Angew. Chem.* **2000**, *112*, 1301; *Angew. Chem. Int. Ed.* **2000**, *39*, 1246.
[22] G. A. Landrum, R. Dronskowski, *Angew. Chem.* **2000**, *112*, 1598; *Angew. Chem. Int. Ed.* **2000**, *39*, 1560.
[23] S. F. Matar, A. Mavromaras, *J. Solid State Chem.* **2000**, *1*, 4.
[24] M. Born, J. E. Mayer, *Z. Phys.* **1932**, *75*, 1.
[25] D. G. Pettifor, R. Podloucky, *Phys. Rev. Lett.* **1984**, *53*, 1080.
[26] J. K. Burdett, S. Lee, *J. Am. Chem. Soc.* **1985**, *107*, 3063.
[27] L. M. Hoistad, S. Lee, *J. Am. Chem. Soc.* **1991**, *113*, 8216.
[28] S. Lee, *Acc. Chem. Res.* **1991**, *24*, 249.
[29] G. Kresse, J. Hafner, *Phys. Rev. B* **1993**, *47*, 55.
[30] G. Kresse, J. Hafner, *Phys. Rev. B* **1994**, *49* 14251.
[31] G. Kresse, J. Furthmuller, *Comput. Mater. Sci.* **1995**, *6*, 15.
[32] G. Kresse, J. Furthmuller, *Phys. Rev. B* **1996**, *54* 11169.
[33] D. Vanderbilt, *Phys. Rev. B* **1990**, *41*, 7892.
[34] H. J. Monkhost, J. F. Pack, *Phys. Rev. B* **1976**, *13*, 5188.
[35] P. E. Blöchl, O. Jepsen, O. K. Andersen, *Phys. Rev. B* **1994**, 49, 16223.
[36] J. P. Perdew, Y. Wang, *Phys. Rev. B* **1991**, *45*, 13244.
[37] N. D. Mermin, *Phys. Rev. A* **1965**, *137*, 1441.
[38] A. D. Vita, M. J. Gillan, *J. Phys. Condens. Matter* **1992**, *4*, 599.
[39] M. Methfessel, A. T. Paxton, *Phys. Rev. B* **1989**, *40* 3616.
[40] R. E. Cohen, M. J. Mehl, D. A. Papaconstantopoulos, *Phys. Rev. B* **1994**, 50, 14694.
[41] M. J. Mehl, D. A. Papaconstantopoulos, *Phys. Rev. B* **1996**, *54*, 4519.
[42] J. Cerdá, F. Soria, *Phys. Rev. B* **2000**, *61*, 7965.
[43] W. M. C. Foulkes, R. Haydock, *Phys. Rev. B* **1989**, *39*, 12520.
[44] R. E. Cohen, L. Stixrude, E. Wasserman, *Phys. Rev. B* **1997**, *56*, 8575.
[45] P. Ordejón, *Comput. Mater. Sci.* **1998**, *12*, 157.
[46] J. Ortega, *Comput. Mater. Sci.* **1998**, *12*, 192.
[47] T. Frauenheim, G. Seifert, M. Elstner, S. Hainal, G. Jungnickel, D. Porezag, S. Suhai, R. Scholz, *Phys. Status Solidi* **2000**, *217*, 41.
[48] M. Elstner, T. Frauenheim, E. Kaxiras, G. Seifert, S. Suhai, *Phys. Status Solidi* **2000**, *217*, 357.
[49] M. Wolfsberg, L. Helmholz, *J. Chem. Phys.* **1952**, *20*, 837.

[50] R. H. Summerville, R. Hoffmann, *J. Am. Chem. Soc.* **1976**, *98*, 7240.
[51] D. G. Pettifor, *Solid State Phys.* **1987**, *40*, 43.
[52] R. Rousseau, S. Lee, *J. Chem. Phys.* **1994**, 101, 10753.
[53] F. A. Cotton, G. Wilkinson, *Advanced Inorganic Chemistry*, 3rd ed., Interscience, New York, **1972**.
[54] K. S. Pitzer, *Acc. Chem. Res.* **1974**, *12*, 271.
[55] P. Villars, L. D. Calvert, *Pearson's Handbook of Crystallographic Data for Intermetallic Phases*, American Society for Metals, Metal Park, OH, **1991**.
[56] J. H. Rose, J. R. Smith, F. Guinea, J. Ferrante, *Phys. Rev. B* **1984**, *29*, 2963.
[57] J. K. Burdett, *Struct. Bond.* **1987**, *65*, 29.
[58] U. Häusermann, R. Nesper, *J. Alloys Compd.* **1995**, *218*, 244.
[59] R. Rousseau, J. S. Tse, *Prog. Theor. Phys. Suppl.* **2000**, *138*, 47.
[60] J. S. Tse, K. Uehara, R. Rousseau, A. Ker, C. I. Ratcliffe, M. A. White, G. Mackay, *Phys. Rev. Lett.* **2000**, *85*, 114.
[61] J. S. Tse, G. Frapper, A. Ker, R. Rousseau, D. D. Klug, *Phys. Rev. Lett.* **1999**, *82*, 4472.
[62] *Binary Alloy Phase Diagrams*, 2nd ed. (Eds.: T. B. Massalski, H. Okamoto, P. R. Subramanian), American Society for Metals, Metal Park, OH, **1990**.
[63] From 7–8 $e^-$ per atom, the preferred structure for unordered alloys and for the elements is the hcp structure. However, for ordered alloys the fcc arrangement is also found in this region. For example, cubic $AuCu_3$, an ordered variant of the fcc arrangement, is often found between 7–8 $e^-$ per atom. Examples include $NbRu_3$, $IrMn_3$, $HfRh_3$, $TiIr_3$, $TiRh_3$, $PtMn_3$, $RhMn_3$, $TiCo_3$, and $ZrIr_3$.
[64] By making this choice of cell, it should be noted we are explicitly disallowing both the hcp and dhcp structures. The subject of hcp, dhcp, and fcc ordered transition metal alloys is one rich in structures. Common structure types found are the $TiAl_3$ and $AuCu_3$, both ordered arrangements of an fcc array of atoms, $SnTi_3$ and $TiAl_3$ structure types, both ordered arrangements of an hcp array of atoms, and $TiNi_3$, an ordered arrangement of dhcp. The methods described in this paper apparently are capable of sorting the energetic differences between these structures. As these results do not properly fit with this article we reserve this discussion for a subsequent paper.
[65] J. K. Burdett, *Chemical Bonding in Solids*, Oxford, New York, **1995**.

Received: December 11, 2000 [F2923]

  0947-6539/01/0712-2662 $ 17.50+.50/0 